第33卷 第9期 焊 接 学 报 Vol. 33 No. 9
2012年9月 TRANSACTIONS OF THE CHINA WELDING INSTITUTION September 2012

气体熔池耦合活性TIG焊方法

黄 勇[1,2]， 刘瑞琳[2]， 樊 丁[1,2]， 康再祥[1]， 郝延召[2]， 瞿怀宇[2]
(1. 兰州理工大学 甘肃省有色金属新材料省部共建国家重点实验室，兰州 730050;
2. 兰州理工大学 有色金属合金及加工教育部重点实验室，兰州 730050)

摘 要：提出了一种新型活性TIG焊方法——气体熔池耦合活性TIG焊，即GPCA-TIG焊. 该焊接方法将气体分两层流动，内层气体采用惰性气体起到保护熔池的作用；外层气体则为含活性元素O的气体，将活性元素O引入熔池金属，达到增加熔深的目的. 文中以SUS304不锈钢为焊接母材，研究了GPCA-TIG焊接法对焊接电弧及焊缝成形的作用，以及该方法主要工艺参数对焊缝熔深和深宽比的影响. 结果表明，在相同参数下，与常规TIG焊方法相比，GPCA-TIG焊可不开坡口一次性焊透8 mm不锈钢板，焊接效率明显提高. 同时采用该方法，可以有效避免钨极的氧化烧损.

关键词：GPCA-TIG焊；气体熔池耦合；外层气体；O元素
中图分类号：TG444 文献标识码：A 文章编号：0253-360X(2012)09-0013-04


黄 勇

0 序 言

钨极氩弧焊(tungsten inert gas welding，TIG焊)是现代工业制造中广泛采用的一种惰性气体保护焊，是常规焊接方法中高质量焊接的代表，特别适用于不锈钢和钛、铝、镁及其合金的焊接. 但常规TIG焊完成单道焊一次成形的板厚小，一般在4 mm以下. 活性焊是一种深熔深高效焊接方法，20世纪60年代由乌克兰巴顿焊接研究所[1,2]首先提出. 目前活性焊中研究最广泛并得到工业应用的是A-TIG(activating flux TIG)焊，它通过在常规TIG焊前将很薄的一层表面活性剂涂覆在施焊板材表面可使得焊接熔深显著增加，达到常规TIG焊的2~3倍. 该方法具有焊接效率高，焊缝质量较好等优点. 但因存在着针对于不同母材金属需要开发相应的专用活性剂材料和活性剂涂覆工艺较为复杂等不足，在一定程度上限制了它的进一步发展.

A-TIG焊的研究表明，对于碳钢和不锈钢等铁系合金而言，O等活性元素改变熔池表面张力温度系数是活性剂增加焊缝熔深的主要机理[3-6]. 文中通过改变活性元素的引入方式，提出了一种新型活性焊接方法—气体熔池耦合活性(gas pool coupled activating，GPCA)焊，该方法采用内外喷嘴将含活性元素O的气体与惰性气体分开，内层为惰性气体，保护熔池和钨极，外层气体则为含活性元素O的单一或者混合气体，通过电弧的作用分解出O元素，在熔池周边低温区域引入活性元素O. 因内喷嘴的外壁是向内有一小角度的倾斜，而外喷嘴下端的内壁是直壁，因此可以通过调节外喷嘴相对于内喷嘴的上升高度实现调节外层气体与熔池的耦合程度，外喷嘴的上升高度越小耦合度越大. 该方法可以微量调节进入熔池表面的活性元素O，达到控制熔池Marangoni对流方式，显著增加焊接熔深的目的. 与A-TIG焊相比，该方法避免了活性剂材料开发，去除了活性剂手工涂覆工序，并提高了焊接过程稳定性，实现了自动化焊接. 与通过活性混合气体引入活性元素O的活性焊接方法相比，该方法可通过调节外层气体与熔池的耦合程度微量调节活性元素O进入熔池的含量，不需要高精度的气体配比器，降低了设备成本，实用性更强. 该方法可适用于TIG焊、MIG焊、等离子弧焊等焊接方法.

文中将GPCA焊应用于不锈钢TIG焊，与常规TIG焊比较，研究焊接电弧、电弧电压、焊缝成形以及钨极形貌的变化及其主要工艺参数对焊缝成形的影响规律，这对于推动该方法的研究和应用具有重要的意义.

1 试验方法

采用GPCA-TIG焊方法，即气体熔池耦合活性

收稿日期：2011-07-25
基金项目：国家自然科学基金资助项目(51074084)；甘肃省自然科学基金资助项目(1010RJZA037)

TIG 焊，进行工件表面熔焊．焊接采用专用 GPCA-TIG 焊枪，内层保护气体为氩气，外层为含活性元素 O 的气体．母材金属为 SUS304 奥氏体不锈钢，板厚为 8 mm．

焊接前先用丙酮擦拭工件表面以除去表面油污，然后用砂纸清理表面，直到露出金属光泽为止．待焊件冷却至室温后，进行取样、打磨和腐蚀，比较常规 TIG 焊与 GPCA-TIG 焊焊缝熔深和深宽比的变化以及采用不同焊接方法焊接后对钨极形貌的影响，研究了 GPCA-TIG 焊主要工艺参数对焊缝成形的影响．

GPCA-TIG 焊接工艺参数为焊接电流 160 A，焊接速度 60 mm/min，钨极伸出长度3 mm，弧长 2 mm，内层气体为氩气，气体流量为 10 L/min，外层气体为 O_2，气体流量为 5 L/min，外喷嘴上升高度为 0 mm．常规 TIG 焊的焊接工艺参数，除了氩气气体流量为 GPCA-TIG 焊内外两层气体流量之和以外，其余与 GPCA-TIG 焊的相同．

2　试验结果

2.1　电弧形态

图1 给出了焊接电弧形态．如图1 所示，GPCA-TIG 焊时焊接过程稳定，电弧均为典型的钟罩形态．与常规 TIG 焊相比，GPCA-TIG 焊电弧的外围收缩明显，二者电压分别为 12.7，15.5 V．

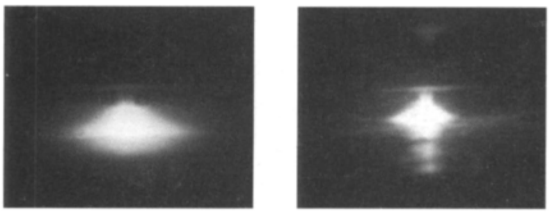

(a) 常规TIG焊　　(b) GPCA-TIG焊

图1　焊接电弧形态

Fig. 1　Arc shapes

2.2　焊缝表面形貌

焊缝表面形貌如图 2 所示，GPCA-TIG 焊焊缝表面成形良好，波纹细腻．与常规 TIG 焊相比，焊缝表面存在一层氧化渣，焊缝宽度明显变窄．

2.3　焊缝截面形貌

焊缝横截面形貌如图 3 所示，可以看出，常规 TIG 焊焊缝宽而浅，熔深为 2.06 mm，深宽比为 0.21，而 GPCA-TIG 焊焊缝深而窄，在该参数下能将 8 mm后不锈钢板不开坡口一次性焊透，深宽比为

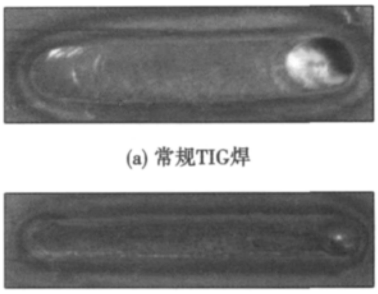

(a) 常规TIG焊

(b) GPCA-TIG焊

图2　焊缝表面形貌

Fig. 2　Weld surface appearances

1.06．GPCA-TIG 焊焊缝内未发现氧化物夹杂和气孔等缺陷存在．

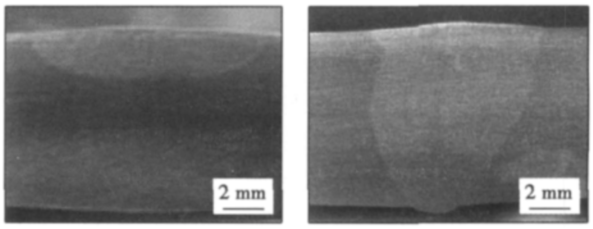

(a) 常规TIG焊　　(b) GPCA-TIG焊

图3　焊缝横截面形貌

Fig. 3　Cross-section appearance of weld

2.4　焊后钨极形貌

图4 比较了 3 种焊接方法对钨极表面的氧化情况．由图4 可以看出，单层 Ar + 10% O_2 混合气体保护钨极电弧焊时，与常规 TIG 焊相比，焊后钨极表面氧化严重，如图4c 所示．而采用 GPCA-TIG 焊时，尽管外层气体中 O_2 含量高达 100%，钨极表面在焊接

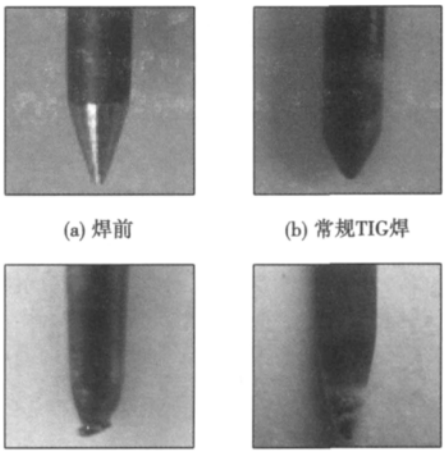

(a) 焊前　　(b) 常规TIG焊

(c) Ar+10%O_2　　(d) GPCA-TIG焊

图4　钨极氧化程度比较

Fig. 4　Oxidation degree of tungsten electrode after welding

过程中依然得到了良好的保护，几乎没有被氧化，如图 4d 所示，与常规 TIG 焊焊后钨极形貌相似.

2.5　工艺参数对焊缝成形的影响

2.5.1　外喷嘴上升高度的影响

图 5 为外喷嘴不同的上升高度时焊缝截面形貌. 如图 5 所示，随着外喷嘴高度的上升，焊缝熔深逐渐递减. 因为随着外喷嘴高度的上升，外层气体与熔池的耦合度随之减小，即单位时间内过渡到熔池金属的活性元素 O 也随之减少. 在该参数下外喷嘴相对于内喷嘴上升高度从 0 mm 调节到 3 mm，其熔深和深宽比变化规律如图 6 所示.

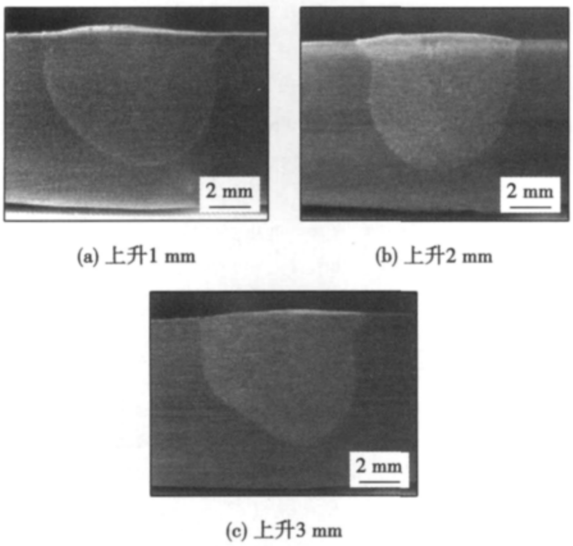

图 5　外喷嘴不同的上升高度时焊缝截面形貌
Fig. 5　Weld penetration under different heights of outer nozzle

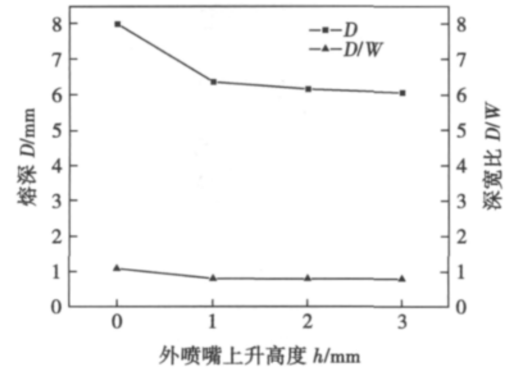

图 6　外喷嘴上升高度对焊缝熔深及深宽比的影响
Fig. 6　Effect of outer nozzle with different heights on weld depth and D/W ratio

2.5.2　不同外层气体种类对焊缝熔深的影响

改变外层气体的种类，分别采用 CO_2 和氩气，其它焊接参数不变，如图 7a 所示，当外层气体通以 CO_2 时，焊缝熔深为 7.5 mm，深宽比为 0.84，其作用与 O_2 类似，均能向熔池过渡活性元素 O，改变熔池的 Marangoni 对流方式，显著增加熔深. 当外层气体通以氩气时，熔深为 2.02，深宽比为 0.18，如图 7b 所示，其成形与常规 TIG 焊相似，表明氩气分层流动后对 GPCA-TIG 焊焊缝成形无影响.

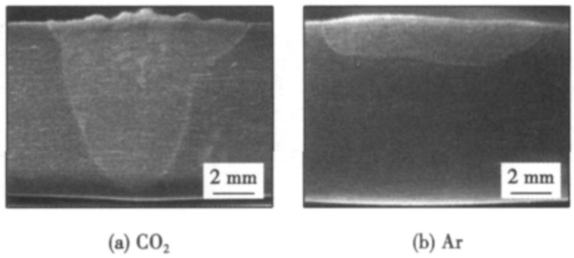

图 7　外层气体种类对焊缝熔深熔宽的影响
Fig. 7　Effect of outer gas on weld penetration and weld width

2.5.3　内层气体流量的影响

图 8 为不同内层气体流量(q)时焊缝截面形貌. 如图 8 所示，随着内层保护气体流量增大，焊缝熔深先增加后减少，其熔深和深宽比变化如图 9 所示. 从文中试验结果可以看出，内层气体的流量过小或过大时，会导致外层气体与熔池的耦合程度过大或过小，从而使得熔深随着内层气体流量的增加呈现先增大后减小的趋势，这主要是因为在相同温度下，表面张力温度系数随 O 含量的增加而增加，由负值变为正值，而当 O 含量超过临界范围后，熔池表面张力温度系数又由正变负所致[7].

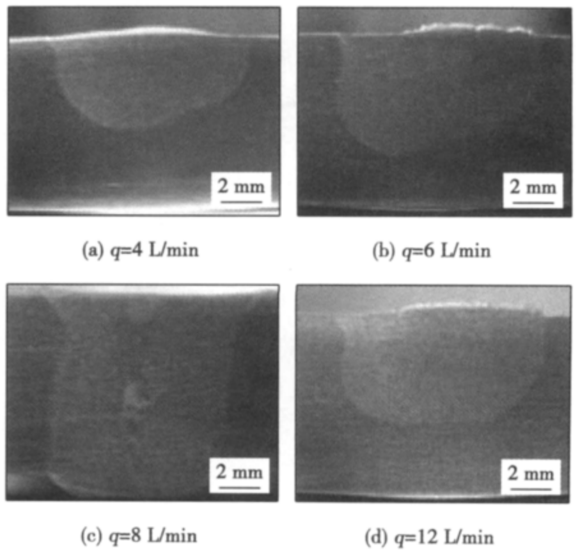

图 8　不同内层气体流量时焊缝截面形貌
Fig. 8　Weld penetration under different flow rate of inner gas

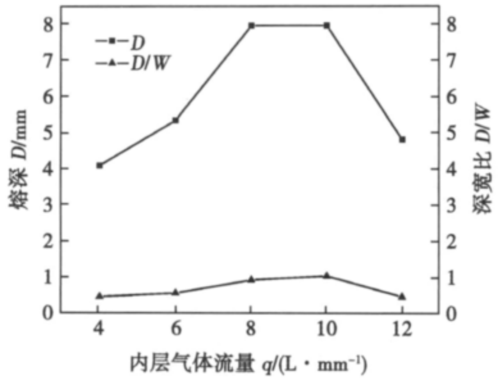

图9 内层气体流量对焊缝熔深及深宽比的影响

Fig. 9 Effect of different inner gas flow rates on weld depth and D/W ratio

3 分析与讨论

关于活性元素增加不锈钢TIG焊熔深的机理，越来越多的人认为熔池金属表面张力温度系数改变是其主要机理. Heiple等人[8]认为，表面活性元素(如O,S等)可降低熔池金属表面张力，当熔池中存在表面活性元素时，可使熔池表面张力温度系数由负值变为正值，改变Marangoni对流方向，显著增加熔深. Sahoo等人[9]得到了Fe-O二元合金中熔池表面张力与温度和活性元素含量关系的半经验公式，由该公式可得出在不同氧含量下熔池表面张力温度系数随温度变化的曲线. 这些研究表明，活性元素可以降低金属的表面张力，其作用与温度有关，当在金属熔点以上的较低温度时，活性元素降低金属表面张力的作用最明显. 基于以上理论，文中提出了GPCA-TIG焊接方法，将活性元素O通过电弧外围区域引入并通过与熔池金属耦合，将其引入到熔池周边较低温度区域，强烈降低熔池金属表面张力，而熔池中心高温区域不引入活性元素O，表面张力不变，以此更加有效地增大表面张力温度系数，使得熔池周边区域的表面张力大大低于熔池中心区域，形成更加强烈的由熔池边缘向熔池中心区域的Marangoni对流，更加有效地将电弧热量传向熔池底部，形成窄而深的焊缝. 由文中试验结果可以看出，GPCA焊确实能有效实现全自动深熔深高效焊接. 同时GPCA-TIG焊接电弧与TIG焊相比较，电弧有一定收缩，电压值也较TIG焊升高了2.8 V，这可能有二方面的原因. 一是GPCA-TIG焊使气体分成内外两层流动，与常规TIG焊相比，外层气体冷却使得电弧发生收缩; 二是在焊接过程中在焊缝表面形成的一层氧化层使得电弧发生收缩. 但究竟是何种原因导致的电弧收缩，电弧收缩后对焊缝成形的影响以及能否促进熔深的增加还需要进一步的研究与论证.

4 结 论

(1) 与传统TIG焊相比，采用GPCA-TIG焊方法，熔宽明显收缩，焊缝表面成形良好，可不开坡口一次焊透8 mm厚不锈钢板. 同时避免焊接过程中钨极的氧化烧损.

(2) 通过调节外喷嘴的上升高度可微量调节外层活性气体向熔池金属过渡活性组元氧的含量.

(3) 焊缝熔深随内层保护气体流量的增加，先增加后减少.

参考文献:

[1] Lucas W, Howse D S. Activating flux increasing the performance and productivity of the TIG and plasma processes [J]. Welding and Metal Fabrication, 1996, 64(1): 11-17.

[2] Mkara A M. High-tensile martensitic steels welded by argon tungsten arc process using flux [J]. Automatic Welding, 1968, 21(7): 78-79.

[3] 黄 勇，樊 丁，林 涛，等. 不锈钢电弧辅助活性TIG焊[J]. 焊接学报. 2009, 30(10): 1-4.
Huang Yong, Fan Ding, Lin Tao, *et al*. Arc assisted activation TIG welding process for stainless steels [J]. Transactions of the China Welding Institution, 2009, 30(10): 1-4.

[4] Fujii H, Sato T, Lu S P, *et al*. Development of an advanced A-TIG(AA-TIG) welding method by control of Marangoni convection [J]. Materials Science and Engineering A, 2008, 495(1/2): 296-303.

[5] 樊 丁，林 涛，黄 勇，等. 电弧辅助活性TIG焊接法[J]. 焊接学报，2008, 29(12): 1-4.
Fan Ding, Lin Tao, Huang Yong, *et al*. Arc assisted activating TIG welding process [J]. Transactions of the China Welding Institution, 2008, 29(12): 1-4.

[6] 陆善平，李冬杰，李殿中，等. 双层气流保护TIG焊接方法[J]. 焊接学报，2010, 31(2): 21-24.
Lu Shanping, Li Dongjie, Li Dianzhong, *et al*. Double shielded TIG welding method [J]. Transactions of the China Welding Institution, 2010, 31(2): 21-24.

[7] Heiple C R, Roper J R, Stanger R T, *et al*. Surface active element effects on the shape of GTA, laser and electron beam welds [J]. Welding Research Supplement, 1983, 62(3): 72-77.

[8] Heiple C R, Roper J R. Mechanism for minor element effect on GTA fusion zone geometry [J]. Welding Journal, 1982, 61(4): 97-102.

[9] Sahoo P, Debroy T. Surface tension of binary metal-surface active solute systems under conditions relevant to welding metallurgy [J]. Metallurgical Transactions, 1987, 19(6): 483-491.

作者简介: 黄 勇，男，1972年出生，副教授，博士. 主要从事高效焊接技术研究. 发表论文40余篇. Email: hyorhot@lut.cn

MAIN TOPICS,ABSTRACTS & KEY WORDS

Visualized diagnosis for metallic parts deposition shaping quality ZHANG Haiou[1], QIU Lipeng[1], RUI Daoman[1], WANG Guilan[2], YU Yang[1] (1. State Key Laboratory of Digital Manufacturing Equipment and Technology, Huazhong University of Science and Technology, Wuhan 430074, China; 2. State Key Laboratory of Material Processing and Die & Mould Technology, Huazhong University of Science and Technology, Wuhan 430074, China). pp 1 - 4

Abstract: Single-camera vision was used to monitor the deposition manufacturing process. By using of image processing technology, the deposition morphology information was processed to get the deposition width. The defect position was calculated by virtue of the spatial orientation mathematical model, which takes the defect pixel coordinate as the source. In the end, the experiment to monitor the deposition was carried out. The experimental results show that the mathematical model and the image processing arithmetic can monitor the deposition width precisely without contact. The method also can recognize and locate the possible defect point fleetly and accurately. Thus the method can adjust and optimize the technological parameter of the deposition to ensure the shape precision and the dimensional precision of the part.

Key words: deposition shaping; image process; deposition contour recognition; deposition width monitoring; defect location

Experimental study on fracture toughness of butt weld of Q460C high-strength structural steel WANG Yuanqing[1], LIN Yun[2], ZHANG Yannian[2], SHI Yongjiu[1] (1. Key Laboratory of Civil Engineering Safety and Durability, China Education Ministry, Tsinghua University, Beijing 100084, China; 2. School of Civil Engineering, Shenyang Jianzhu University, Shenyang 110168, China). pp 5 - 8

Abstract: Three point bending (TPB) fracture toughness tests of weld zone and heat affected zone of Q460C structural high-strength steel with 14 mm in thickness at distinct low temperature points were carried out, and the fracture toughness values for weld zone and heat affected zone of the specimens were obtained. Then regression analysis with Boltzmann function was used, then the ductile-brittle transition temperature and its variation with temperature were acquired. The TPB fracture appearance was analyzed with the scanning electron microscope. The results showed that low temperature had obvious influence on the fracture toughness of weld zone and heat affected zone of Q460C steel. With the temperature decreasing, there was a downward trend on the fracture toughness. Moreover, the ductile-brittle transition temperature of weld zone is about −53.6 ℃, and that of the heat affected zone was about −40.3 ℃. Besides, the fracture appearances of weld zone and heat affected zone fractured at temperature point below −20 ℃ showed the brittle characteristics significantly.

Key words: high strength steel; fracture toughness; welded joint; crack tip opening displacement

Interfacial microstructure and bonding strength of diffusion bonded TiAl/Ti/Nb/GH99 alloy joint LI Haixin, WEI Hongmei, HE Peng, FENG Jicai (State Key Laboratory of Advanced Welding and Joining, Harbin Institute of Technology, Harbin 150001, China). pp 9 - 12

Abstract: Diffusion bonding of TiAl-based alloy to Ni-based alloy using Ti/Nb composite interlayer was carried out. The formation phases and the interfacial microstructure of the joints were investigated by scanning electron microscopy, electron probe X-ray analysis and X-ray diffraction. The bonding strength of the joints was evaluated through shear test. The results show that the typical interfacial microstructure of the joint is GH99/$(Ni, Cr)_{ss}$/Ni_3Nb/Ni_6Nb_7/$(Ti, Nb)_{ss}$/α-Ti + $(Ti, Nb)_{ss}$/Ti_3Al/TiAl. The maximum shear strength of 273.8 MPa can be achieved under the condition of $T = 900$ ℃ for $t = 30$ min and $p = 20$ MPa. With the joining temperature T increasing, the interfacial microstructure and thickness of reaction layer changes. When the brazing temperature $T > 900$ ℃, Ni_6Nb_7 reaction layer which has bad effect on the bonding strength forms. Based on the experimental results, the formation process of reaction layer was analyzed and interfacial reaction mechanism of the interface of GH99/Nb and Nb/Ti/TiAl was revealed.

Key words: diffusion bonding; interfacial microstructure; shear strength

Gas pool coupled activating TIG welding method HUANG Yong[1,2], LIU Ruilin[2], FAN Ding[1,2], KANG Zaixiang[1], HAO Yanzhao[2], QU Huaiyu[2] (1. State Key Laboratory of Gansu Advanced Non-ferrous Metal Materials, Lanzhou University of Technology, Lanzhou 730050, China; 2. Key Laboratory of Non-ferrous Metal Alloys and Processing, the Ministry of Education, Lanzhou University of Technology, Lanzhou 730050, China). pp 13 - 16

Abstract: A new welding method named gas pool coupled activating TIG welding was proposed, which contains two layers of shielding gas. The inner inert gas can protect the molten pool, and the outer active gas can provide active element into the molten pool to obtain narrow and deep weld. By taking SUS304 stainless steel as based metal, the effect of GPCA-TIG method on welding arc and weld appearances was studied. In addition, the effect of main welding parameters on weld penetration and D/W ratio was also studied. The results indicate that at the same welding conditions with the traditional TIG welding, the 8 mm thickness stainless steel can be fully penetrated with GPCA-TIG welding process without making a groove. This method can avoid the oxidation of tungsten electrode in welding process.

Key words: GPCA-TIG welding; gas pool coupled; outer gas; O element